

Alleviating both H_0 and S_8 tensions: early dark energy lifts the CMB-lockdown on ultralight axion

Gen Ye^{1,2*}, Jun Zhang^{3,4†}, and Yun-Song Piao^{1,2,3,5‡}

¹ *School of Fundamental Physics and Mathematical Sciences,*

Hangzhou Institute for Advanced Study, UCAS, Hangzhou 310024, China

² *School of Physics, University of Chinese Academy of Sciences, Beijing 100049, China*

³ *International Center for Theoretical Physics Asia-Pacific, Beijing/Hangzhou, China*

⁴ *Theoretical Physics, Blackett Laboratory,*

Imperial College, London, SW7 2AZ, UK and

⁵ *Institute of Theoretical Physics, Chinese Academy of Sciences,*

P.O. Box 2735, Beijing 100190, China

Abstract

The existence of ultralight axion (ULA) with mass $\mathcal{O}(10^{-26}\text{eV})$ is not favored by the CMB observations in the standard ΛCDM model. We show that the inclusion of early dark energy (EDE) will lift the CMB-lockdown on such ULA, and possibly other forms of dark matter beyond cold dark matter. By performing Monte Carlo Markov Chain analysis, it is found that, as opposed to ΛCDM , the AdS-EDE cosmology (with an Anti-de Sitter phase around recombination) now allows the existence of axion with mass 10^{-26} eV and predicts 6% of the matter in our Universe to be such ULA, which can also help alleviating the S_8 tension in EDE.

PACS numbers:

* yegen14@mailsucas.ac.cn

† zhangjun@ucas.ac.cn

‡ yspiao@ucas.ac.cn

I. INTRODUCTION

Based on the standard cosmological constant cold dark matter (Λ CDM) model, the Planck cosmic microwave background (CMB) data suggests that the current expansion rate of the Universe (Hubble constant) is $H_0 = 67.4 \pm 0.5 \text{ km/s/Mpc}$ [1]. However, using Cepheid-calibrated supernovas, Riess et.al reported $H_0 = 73.2 \pm 1.3 \text{ km/s/Mpc}$ [2], in $\sim 4\sigma$ tension with the Planck result, see also other independent local measurements, e.g.[3]. It has been widely thought that this so-called Hubble tension, if confirmed¹, likely signals new physics beyond Λ CDM [5–8].

The currently promising resolution of the Hubble tension is early dark energy (EDE) [9, 10]. In corresponding scenarios, the EDE component is non-negligible only around matter-radiation equality before recombination, which results in a suppressed sound horizon, so $H_0 \gtrsim 70 \text{ km/s/Mpc}$. In past years, the EDE models have been extensively studied [11–27], see also Refs.[28–30] for early modified gravity, for thorough reviews see e.g Refs.[31, 32]. Furthermore, the existence of an Anti-de Sitter (AdS) phase around recombination can allow a higher EDE fraction (without spoiling fit to CMB, BAO and supernova light curves), so that the corresponding AdS-EDE model can be 1σ consistent with local H_0 measurements, see Refs.[17, 21].

In Ref.[21, 22], it has been found that in such pre-recombination solutions, the relevant cosmological parameters must shift with δH_0 , particularly the shift of $\omega_m = \Omega_m h^2$ scales approximately as $\frac{\delta \omega_m}{\omega_m} \sim 2 \frac{\delta H_0}{H_0}$. More dust-like matter induces more clustering (perturbation growth) in the matter-dominated era, so a higher σ_8 (the amplitude of matter perturbations at $8h^{-1} \text{ Mpc}$ scale) and $S_8 \equiv \sigma_8 \sqrt{\Omega_m/0.3}$. S_8 can be probed by local large scale structure (LSS) observations. Recently, based on the Λ CDM model, the weak lensing measurements and redshift surveys [33–36] report lower S_8 values, see also [37]. At first thought, it seems that the EDE resolutions of the Hubble tension will inevitably suffer inconsistency with local S_8 measurements [38–41] (except [20, 23, 42] for combining Planck low- ℓ and SPTpol data), the so-called S_8 tension, because both larger ω_m and n_s ($\delta n_s \simeq 0.4 \frac{\delta H_0}{H_0}$ [22]) will enhance the matter power spectrum around $k_8 \sim (8/h \text{ Mpc})^{-1}$, see also [43].

¹ Recently, using Tip of the Red Giant Branch (TRGB) calibrated supernova, Ref.[4] have reported a lower value $H_0 = 69.8 \pm 0.6(\text{stat}) \pm 1.6(\text{sys})$, statistically consistent with both CMB and Cepheid values, which might imply uncounted uncertainties in current local observations.

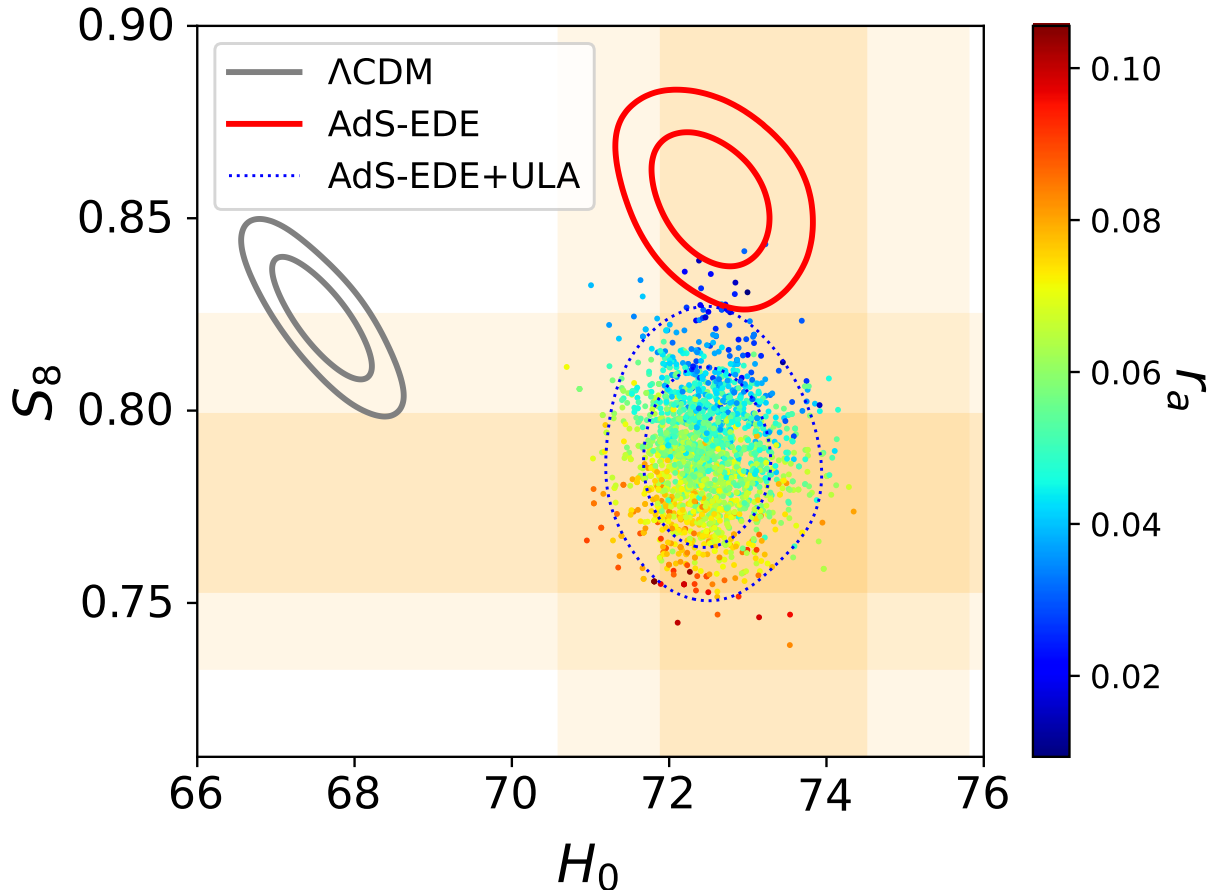


FIG. 1: Posterior distributions of Λ CDM, AdS-EDE and AdS-EDE with ultralight axion (AdS-EDE+ULA) cosmologies in the H_0-S_8 plain. Yellow bands show the 1σ and 2σ region of local $S_8 = 0.755^{+0.019}_{-0.021}$ [33] and $H_0 = 73.2 \pm 1.3$ km/s/Mpc [2] measurements. Scattered points correspond to AdS-EDE+ULA with a color coding for the energy fraction of ULA in total matter $r_a \equiv \Omega_{axion}/\Omega_m$.

However, careful analysis of the physics behind the shift in ω_m tells a different story. The ω_m-H_0 correlation in Ref.[21] is actually the consequence of θ_{CMB} and θ_{BAO} (angular spacing of the acoustic peaks) after recombination being strictly constrained by observations, see also [44], which, however, only relies on the background evolution. In the standard CDM model, $(\omega_m)_{bk} = (\omega_m)_{pt}$, where $(\omega_m)_{bk}$ is the fraction of pressureless ($p \simeq 0$) energy density (relevant to the background evolution) while $(\omega_m)_{pt}$ is the fraction of Jeans-unstable matter (relevant to perturbation growth), thus $\frac{\delta\omega_m}{\omega_m} \simeq 2\frac{\delta H_0}{H_0}$ will suggest exacerbated S_8 tension for EDE. There are, however, other possible DM forms which contribute to $(\omega_m)_{bk}$ and $(\omega_m)_{pt}$ differently. We will show that EDE can indeed accommodate alternative form of

DM, provided certain conditions are met, which will be clarified in the main text.

As an example, the alternative DM form we will consider is the ultra-light axion (ULA), which is theoretically well-motivated and naturally arise from compactifications in string theory [45, 46] and might constitute a fraction of dark matter, see [47] for a recent review. It is interesting that axions with weak self-interaction can lead to black hole superradiance, which can be constrained by black hole spin measurements e.g.[48], polarimetric observations [49], and gravitational wave observations [50–53]. In addition, axion also could be sourced by neutron stars [54–56]. It has been noticed in Ref.[57] that ULA of mass 10^{-26} eV might help alleviate the S_8 tension in EDE. However, Ref.[57] approximated EDE as an effective fluid with an instant transition in its equation of state parameter w as well as the adiabatic sound speed $c_s^2 = w$, which made it hard to see what exact role ULA plays in the cosmic evolution. Besides, the effect of EDE is most prominent when its energy fraction peaks immediately after thawing, at which time $w = \text{const.}$ is not a good approximation since it is the transition phase from $w = -1$ to the final stage.

In this letter we go one step further, treating both EDE and ULA robustly by solving the full background and linearly perturbed Klein-Gordon equations for both fields in the cosmology code². With this improved method, we identified the core DM properties required by EDE to maintain good fit to CMB, which explains why ULA with mass 10^{-26} eV can help with the S_8 tension in EDE. More importantly, our analysis highlights the essential role of EDE in opening the parameter space for alternative DM forms, particularly ULA. The existence of ULA with mass 10^{-26} eV is in fact not favored by Λ CDM, even if the full S_8 related information is included, see [58, 59] and also Fig.2. As we will show in the main text, it is EDE that lifts the CMB lockdown on such DM form.

II. MODEL AND DATASETS

As a phenomenological model, the AdS-EDE potential we will be working with is $V(\phi) = V_0(\phi/M_p)^4 - V_{ads}$, which is glued to a cosmological constant $V(\phi) = \Lambda$ by interpolation [17], where $V_{ads} > 0$ is the AdS depth. It is parameterized by z_c (the redshift at which the field

² Our modified version of CLASS is available at https://github.com/genye00/class_multiscf.git

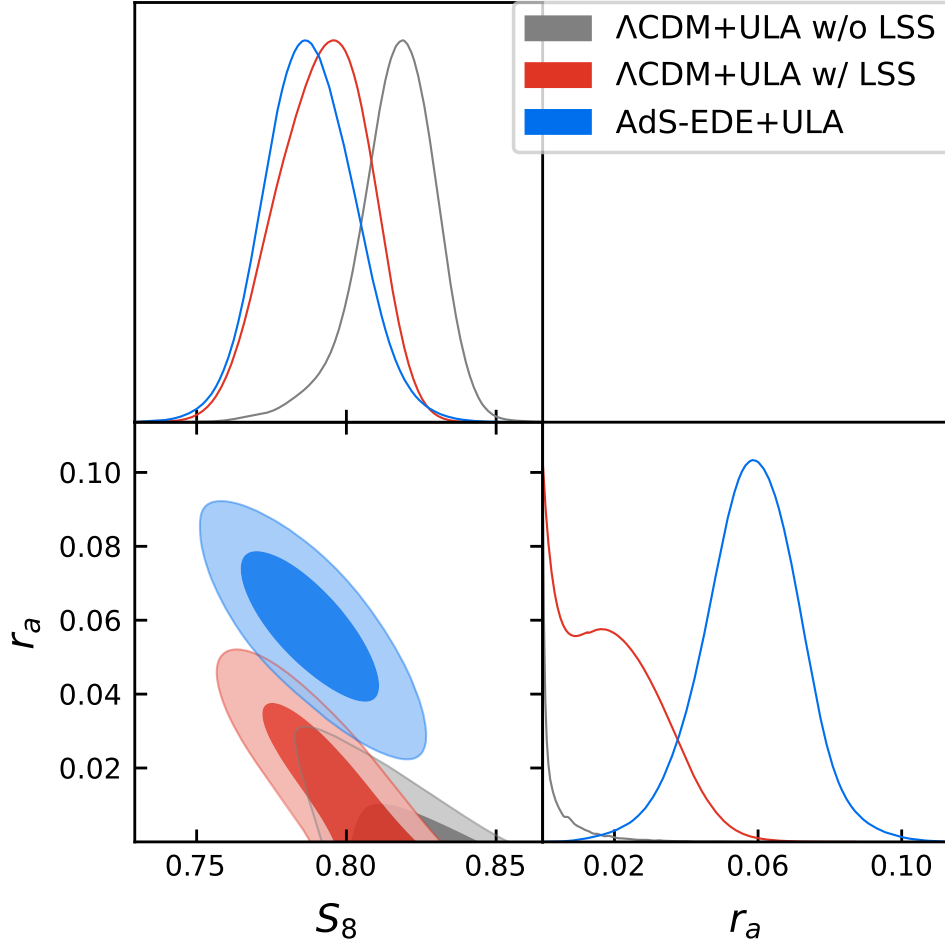


FIG. 2: 68% and 95% posterior distribution of ULA energy fraction $r_a \equiv \Omega_{axion}/\Omega_m$ and S_8 in Λ CDM and AdS-EDE using the baseline+fsBAO+ M_B dataset, see section-II for details. The Λ CDM+ULA w/o LSS result is obtained using P18+BAO+SN+ M_B . Inclusion of S_8 related LSS information only biases the Λ CDM contour to a smaller (larger) value of S_8 (r_a) but does not change the existence conclusion. The ULA used to produce these results has mass $m_a = 1.3 \times 10^{-26}$ eV and coupling constant $f_a \sim 10^{17}$ GeV.

starts rolling), $f_{ede}(z_c)$ (the energy fraction of EDE at z_c) and fixed³ $\alpha_{ads} \equiv V_{ads}/H(z_c) = 3.79 \times 10^{-4}$. Non-zero α_{ads} value effectively puts a theoretical lower bound on f_{ede} and cuts out part of the viable parameter space due to the fact that the field would be trapped

³ According to Ref.[21], the existence of an AdS phase is weakly hinted, see also Appendix-A 2, thus to explore the effect of AdS-EDE we choose to fix the AdS depth α_{ads} to the value in Ref.[17], which is compatible with P18+BAO+SN.

in the disastrous negative energy region if f_{ede} becomes too small. The axion potential is $V(a) = m_a^2 f_a^2 [1 - \cos(a/f_a)]$ with the coupling constant $f_a < M_p$. Theoretically, the initial phase $\Theta_i \equiv a_i/f_a$ of the axion is arbitrary. To reduce the number of free parameters, we fix⁴ the initial phase to the general value $\Theta_i = 2$.

Axion-like scalar field rapidly oscillating around the minimum of its potential mimics a $w = 0$ fluid at the background level while on the perturbation level, it can be effectively regarded as perfect fluid with $c_s^2 \sim \frac{k^2}{4m_a^2 a^2}$, corresponding to the Jeans scale $k_J/a \sim 6^{1/4} \sqrt{H m_a}$ [60–62]. A part of $(\omega_m)_{bk}$ might be constituted of axion $\omega_a = r_a (\omega_m)_{bk}$. To have axion contribute differently to $(\omega_m)_{bk}$ and $(\omega_m)_{pt}$ at the S_8 scale, we must at least have $k_J \lesssim k_8$ at matter-radiation equality, which thus suggests the axion mass $m_a \lesssim \mathcal{O}(10^6 H_0) \sim \mathcal{O}(10^{-26} \text{eV})$. The lower bound on m_a is set by requiring that the axion field mimics matter ($w = 0$) at low redshift. To have an order of magnitude estimation, we require $m_a > 100H(z = 10)$ or equivalently $m_a \gtrsim 2 \times 10^3 H_0 \sim 4h \times 10^{-30} \text{eV}$.

In Fig.3, we plot the evolution of $f_{ede}(z)$ and $f_{axi}(z)$ (the energy fraction of axion), respectively. Here, the EDE field responsible for resolving the Hubble tension thaws at $z = a \text{ few thousand}$, while the axion (equivalently another EDE field with thawing time determined by $m_a = 3H(z)$) making $(\omega_m)_{bk} \neq (\omega_m)_{pt}$ at the S_8 scale thaws well before matter-radiation equality, see also recent Refs.[63, 64] for axion thawing after recombination with $m_a \sim 10^{-29} \text{eV}$.

To calculate linear cosmological perturbations and perform the Monte Carlo Markov Chain (MCMC) analysis, we modified Montepython-3.4 [65, 66] and CLASS [67, 68] to implement the AdS-EDE model and multiple axion species. In particular, for ULA, we solve the full Klein-Gordon equation until it enters the rapidly oscillation phase, specified by $m_a/H \gg 1$, after that we follow Refs.[60–62, 69] and adopt the axion field fluid approximation. Our datasets include:

1. **baseline: P18+SN+BAOLz+S₈.**

P18: The most recent Planck2018 high- l TTTEEE likelihood together with low- l TT, EE and Planck lensing data [70].

⁴ ULA thaws relatively deep ($z \sim 17000$ for the case we studied) in the radiation dominant era, thus Θ_i should only have subdominant effect on the observed CMB provided Θ_i does not take extreme values close to π or 0. See Appendix-A 2 for more details.

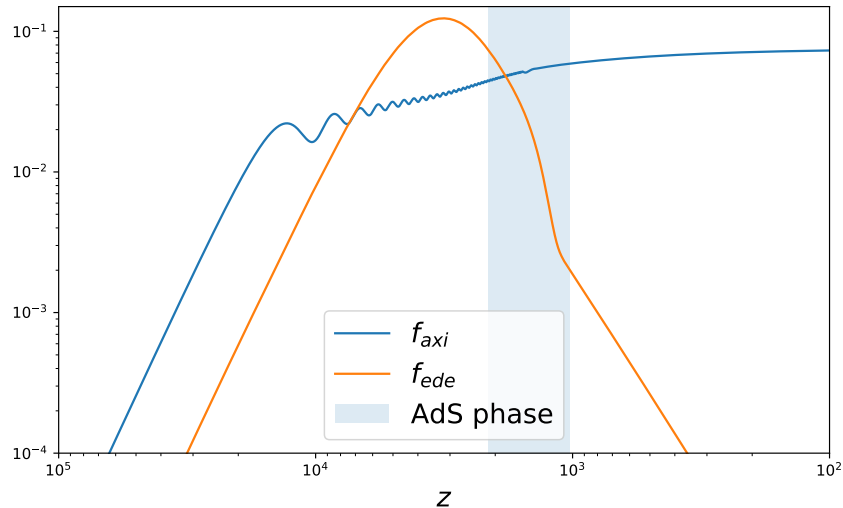


FIG. 3: Evolution of the energy fractions f_{ede} and f_{axi} with respect to redshift in the bestfit AdS-EDE+ULA model. Axion and EDE fields become dynamical at $z \simeq 1.7 \times 10^4$ and $z \simeq 4000$ respectively.

SN: The Pantheon supernova data [71].

BAOLz: The post-reconstructed small- z BAO data from 6dF [72] and MGS [73].

S_8 : The KiDS+VIKING+DESY1 [33] combined result $S_8 = 0.755^{+0.019}_{-0.021}$ is regarded as a Gaussian prior⁵.

2. baseline+EFT/fsBAO+ M_B .

EFT: The full shape galaxy power spectrum data from BOSS DR12 extracted by EFTofLSS [74, 75] (with the publicly available pyBird code [76, 77]), as well as the post-reconstructed BAO data with corresponding covariance matrix.

fsBAO: BOSS DR12 post-reconstructed high- z BAO and redshift space distortion $f\sigma_8$ data with its covariance matrix [78], not independent of EFT.

M_B : In light of Refs.[4, 79–82], the SH0ES result [2], the absolute magnitude of supernovas $M_B = -19.224 \pm 0.042$ mag, is regarded as a Gaussian prior⁶.

⁵ The more recent KiDS-1000 result gives $S_8 = 0.759^{+0.024}_{-0.021}$ [34] and $S_8 = 0.766^{+0.02}_{-0.014}$ for KiDS-1000+BOSS+2dFLenS [35]. The new DES-Y3 reports $S_8 = 0.776 \pm 0.017$ [36]. The Gaussian prior we use is statistically compatible with these updated results.

⁶ In light of Ref.[82]-v1 in arXiv, we take $M_B = -19.224 \pm 0.042$ mag to perform all the MCMC analysis,

Parameters	Λ CDM	AdS-EDE	AdS-EDE+ULA	
	baseline+EFT+ M_B			baseline+fsBAO+ M_B
$100 \omega_b$	$2.248(2.243)^{+0.014}_{-0.015}$	$2.348(2.347)^{+0.016}_{-0.015}$	$2.338(2.331)^{+0.018}_{-0.016}$	$2.335(2.358)^{+0.018}_{-0.017}$
ω_{cdm}	$0.1178(0.118)^{+0.00078}_{-0.00082}$	$0.1312(0.1318)^{+0.0018}_{-0.0017}$	$0.1242(0.1229)^{+0.0023}_{-0.0025}$	$0.1231(0.1239)^{+0.0024}_{-0.0025}$
H_0	$68.81(68.66)^{+0.4}_{-0.38}$	$73.19(73.32)^{+0.51}_{-0.53}$	$72.53(72.14)^{+0.51}_{-0.58}$	$72.48(73.01)^{+0.52}_{-0.57}$
$\ln 10^{10} A_s$	$3.034(3.038)^{+0.015}_{-0.015}$	$3.054(3.051)^{+0.016}_{-0.014}$	$3.063(3.066)^{+0.014}_{-0.015}$	$3.065(3.071)^{+0.014}_{-0.014}$
n_s	$0.9688(0.9668)^{+0.0037}_{-0.0038}$	$0.9976(0.9976)^{+0.0042}_{-0.0039}$	$0.9885(0.9856)^{+0.0048}_{-0.0048}$	$0.9885(0.991)^{+0.005}_{-0.0048}$
τ_{reio}	$0.0533(0.0564)^{+0.007}_{-0.008}$	$0.0499(0.0488)^{+0.0079}_{-0.0075}$	$0.0534(0.0549)^{+0.007}_{-0.0076}$	$0.0540(0.0584)^{+0.0072}_{-0.0074}$
$\ln(1+z_c)$	-	$8.258(8.233)^{+0.1}_{-0.097}$	$8.255(8.256)^{+0.088}_{-0.069}$	$8.246(8.293)^{+0.082}_{-0.068}$
f_{ede}	-	$0.1068(0.1083)^{+0.0043}_{-0.0063}$	$0.1094(0.1124)^{+0.0036}_{-0.0064}$	$0.1116(0.1203)^{+0.0036}_{-0.0084}$
α_{ads}	-	3.79×10^{-4}	3.79×10^{-4}	3.79×10^{-4}
$m_a (10^6 H_0)$	-	-	8.6	8.6
f_a/M_p	-	-	$0.0541(0.0631)^{+0.0081}_{-0.0057}$	$0.0552(0.0597)^{+0.0077}_{-0.0055}$
r_a	-	-	$0.0567(0.0751)^{+0.015}_{-0.013}$	$0.0585(0.0674)^{+0.015}_{-0.013}$
M_B	$-19.39(-19.39)^{+0.011}_{-0.011}$	$-19.26(-19.25)^{+0.015}_{-0.015}$	$-19.27(-19.28)^{+0.014}_{-0.016}$	$-19.27(-19.26)^{+0.014}_{-0.016}$
S_8	$0.808(0.811)^{+0.008}_{-0.009}$	$0.836(0.837)^{+0.01}_{-0.01}$	$0.785(0.772)^{+0.015}_{-0.016}$	$0.788(0.776)^{+0.015}_{-0.016}$
Ω_m	$0.2964(0.2978)^{+0.0048}_{-0.0049}$	$0.2888(0.2888)^{+0.0045}_{-0.0049}$	$0.2975(0.3037)^{+0.0053}_{-0.0057}$	$0.2993(0.2966)^{+0.0052}_{-0.0055}$

TABLE I: Mean and 1σ values of cosmological parameters in AdS-EDE+ULA, as well as the original AdS-EDE model in Ref.[17] and the standard Λ CDM model. The axion mass is $m_a \simeq 1.8h \times 10^{-26}$ eV. Bestfit values are reported in the parenthesis.

III. RESULTS AND ANALYSIS

We fix⁷ the ULA mass to its bestfit value $m_a = 8.6 \times 10^6 H_0 \simeq 1.8h \times 10^{-26}$ eV in AdS-EDE+ULA cosmology with the baseline+EFT+ M_B datasets and perform MCMC analysis over the cosmological parameter set $\{\omega_b, \omega_{cdm}, H_0, \tau_{reio}, \ln 10^{10} A_s, n_s, f_{ede}(z_c), \ln(1+z_c), f_a\}$.

We present in Table-I the mean and bestfit values of cosmological parameters in the best

but in v3 it is changed to $M_B = -19.214 \pm 0.037$ mag. Also, during the revision process of this paper, the SH0ES group reported new result $M_B = -19.253 \pm 0.027$ [83] with Pantheon+ [84]. The difference is statistically marginal and should not significantly affect our results.

⁷ This accelerates convergence and is sufficient for our purpose of studying the cosmological effect of $\sim 10^{-26}$ eV ULA. See Appendix-A 2 for results of varying m_a .

Dataset	Λ CDM	AdS-EDE	AdS-EDE+ULA	
	baseline+EFT+ M_B			baseline+fsBAO+ M_B
Planck18 high- l TTTEEE	2347.70	2354.54	2352.72	2353.82
Planck18 low- l TT	22.87	20.39	20.71	20.87
Planck18 low- l EE	396.32	395.98	396.06	396.59
Planck18 lensing	10.31	10.54	9.82	9.75
Pantheon	1027.12	1027.04	1026.94	1026.89
BAO low z	2.24	3.10	1.53	2.11
BAO high $z + f\sigma_8$	-	-	-	7.14
eft withbao highzNGC	66.48	65.84	69.72	-
eft withbao highzSGC	62.92	64.51	60.73	-
eft withbao lowzNGC	71.14	71.39	71.26	-
S_8	7.89	16.61	1.18	1.06
M_B	12.00	0.05	0.79	0.12
χ_{CMB}^2	2777.2	2781.45	2779.31	2781.03
χ_{EFT}^2	200.54	201.74	201.71	-
χ_{tot}^2	4026.99	4029.99	4011.46	3818.35

TABLE II: Bestfit χ^2 per dataset for AdS-EDE, AdS-EDE+ULA and Λ CDM. The axion mass is $m_a \simeq 1.8h \times 10^{-26}$ eV.

constrained models. For AdS-EDE+ULA, we also present results for baseline+fsBAO+ M_B , which gives very similar cosmological constraints to baseline+EFT+ M_B but converges significantly faster than the latter due to no need of computing loop corrected matter power spectrum for the EFT likelihood. The corresponding bestfit χ^2 per dataset is reported in Table-II. The bestfit model implies an axion field thawing at $z \simeq 1.7 \times 10^4$ with mass $m_a \simeq 1.8h \times 10^{-26}$ eV and coupling constant $f_a \simeq 1.5 \times 10^{17}$ GeV, corresponding to the axion-to-matter ratio $r_a \equiv \Omega_{axion}/\Omega_m \simeq 6.7\%$.

In Fig.1, we see that the addition of an axion field effectively lowers the predicted S_8 value, without interfering with the ability of AdS-EDE to solve the Hubble tension. Interestingly, now $H_0 = 72.53_{-0.58}^{+0.51}$ and $S_8 = 0.785_{-0.016}^{+0.015}$, both are within 1σ bands of the local measurements. According to the baseline+EFT+ M_B columns in Table.II, as opposed

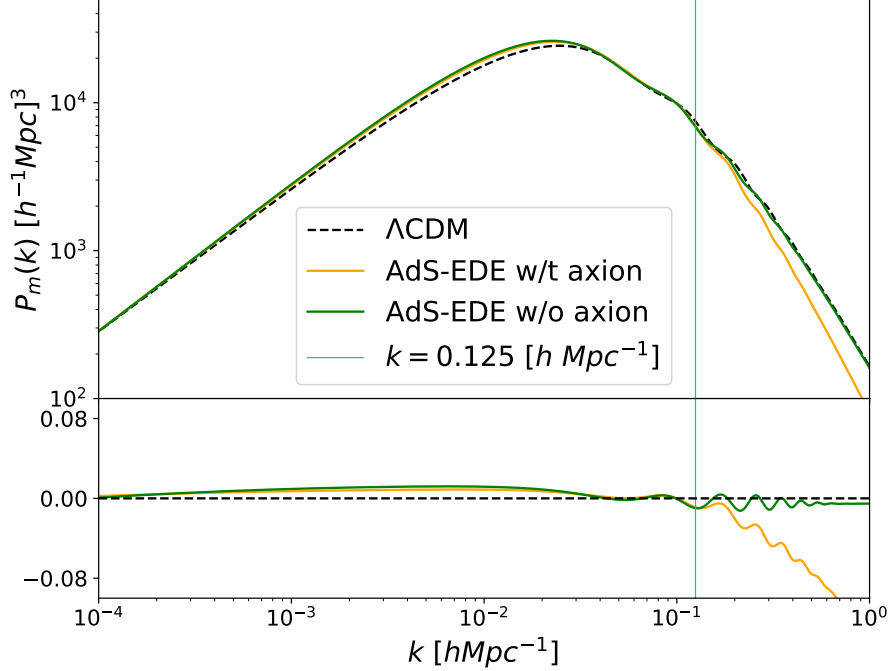


FIG. 4: In the bestfit AdS-EDE and AdS-EDE+ULA models, linear matter power spectrum at $z = 0$ is compared with that in the Λ CDM model.

to previous studies using P18+BAO+SN [17, 21], AdS-EDE now yields obviously worse fit to the CMB data ($\Delta\chi_{CMB}^2 = +4.25$) as well as S_8 prior ($\Delta\chi_{S_8}^2 = +8.72$) compared with Λ CDM, due to the inclusion of LSS related datasets (EFT and S_8) and the exacerbated S_8 tension generic to EDE-like models [39, 40], see also Fig.1. Compared with AdS-EDE alone, inclusion of ULA alleviates the tension in data due to improved $\chi_{S_8}^2$ and χ_{CMB}^2 . Despite the improvement over AdS-EDE alone, AdS-EDE+ULA still does not fit the CMB data as well as Λ CDM, implying some residual tension. To quantify the residual tension, we use the metric $Q_{DMAP}^2 \equiv \chi_{\min, D_1+D_2}^2 - \chi_{\min, D_1}^2 - \chi_{\min, D_2}^2$ from [85, 86], where D_1 and D_2 are two datasets. Taking $D_1 = \text{P18+BAOLZ+SN+EFT}$ and adding the S_8 and M_B prior one at a time we get $Q_{DMAP} = 4.5$ for $D_2 = S_8$, $Q_{DMAP} = 0.9$ for $D_2 = M_B$ and $Q_{DMAP} = 5.1$ for $D_2 = S_8 + M_B$ in the AdS-EDE+ULA model, where we have assumed $\chi_{\min, D_2}^2 = 0$ since D_2 contains at most two data points. See Appendix-A 1 for details. r_a is clearly negatively correlated with S_8 , since larger r_a will bring larger suppression of matter perturbations on the S_8 scale, see Fig.4.

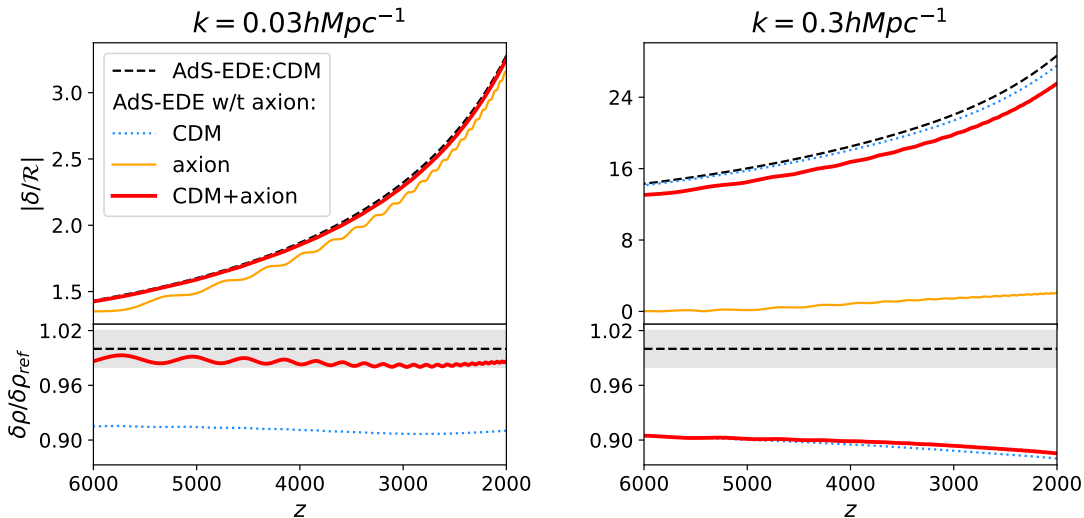


FIG. 5: Density perturbation for axion and CDM in the bestfit AdS-EDE and AdS-EDE+ULA models. Upper panels plot the relative density perturbation $\delta \equiv \delta\rho/\rho$, normalized to the primordial curvature perturbation \mathcal{R} . Lower panels plot the density perturbations with $\delta\rho_{ref} \equiv \delta\rho_{cdm}$ in the AdS-EDE model. Gray band stands for 2% relative variation around the bestfit AdS-EDE model.

In Table-I, the AdS-EDE+ULA model predicts lower $\omega_{cdm} \simeq 0.124$ compared with $\omega_{cdm} > 0.13$ in the original AdS-EDE. As pointed out by Ref.[21], the background CMB+BAO compatibility requires a larger ω_m . This must be achieved in a way compatible with the full anisotropic CMB dataset. EDE adds to the total amount of Jeans stable species before recombination. Thus to have the correct amount of radiation driving and early ISW, the amount of clustering species has to be increased accordingly [21, 43]. Assuming DM is entirely consisted of CDM, the majority of the needed increase in clustering species then must be realized by CDM, shifting ω_{cdm} in EDE cosmologies to a considerably larger value than Λ CDM, enhancing the matter power spectrum on small scales and exacerbating the S_8 tension. This is identified as a difficulty of EDE in Ref.[38–41]. However, from another point of view, this might also be an implication of additional DM forms beyond CDM in EDE. The key property of these potential new DM forms is that they must act as Jeans unstable species on the relevant scales to compensate for the EDE pressure support. In AdS-EDE+ULA, this role is played by the ULA, thus a lower ω_{cdm} is predicted. Additionally, ULA behaves as matter on the background level (i.e. $\rho_a \propto a^{-3}$) so Ω_m is nearly unchanged compared with Λ CDM in Table.I, saturating the bound reported in Ref.[21]. The effect

of EDE is only significant at scales entering horizon near z_c when the EDE field is non-negligible, roughly corresponding to the first acoustic peak ($l \lesssim 300$). Thus one expects $k_{J,eq} \gtrsim \mathcal{O}(0.01)\text{Mpc}^{-1}$ which disfavors $m_a \lesssim \mathcal{O}(10^{-27}\text{eV})$. Recall from previous section that for ULA to have effect on the S_8 tension, we need $m_a \lesssim \mathcal{O}(10^{-26}\text{eV})$, implying a mass range of interest $\mathcal{O}(10^{-26}\text{eV}) \gtrsim m_a \gtrsim \mathcal{O}(10^{-27}\text{eV})$. The axion mass $m_a = 8.6 \times 10^6 H_0 \simeq 1.8h \times 10^{-26}\text{eV}$ used to perform the MCMC analysis is within this mass range and corresponds to $k_{J,eq} \sim 0.16h\text{Mpc}^{-1}$, well above the EDE relevant scale. In Fig.5, we clarify this keypoint by plotting the density perturbations for axion and CDM near z_{eq} for $k_{EDE} = 0.03h\text{Mpc}^{-1}$ and $k_{LSS} = 0.3h\text{Mpc}^{-1}$, respectively. At k_{EDE} , axion mimics CDM in terms of perturbation growth and together with the actual CDM, they produce correct amount of $\delta\rho$ for clustering species as required by the AdS-EDE bestfit (left panel of Fig.5). Around the LSS relevant scales, axion suppresses clustering (right panel of Fig.5).

IV. CONCLUSION

We argued that the increase in ω_m and clustering species required by EDE might be a possible indication of additional DM forms beyond CDM. We studied a well-established example of DM, the ULA, in EDE and showed explicitly by performing MCMC analysis that, as opposed to ΛCDM , AdS-EDE can indeed accommodate non-negligible amount ($\sim 6\%$) of ULA with mass $m_a \simeq 1.3 \times 10^{-26}\text{eV}$ and coupling constant $f_a \simeq 1.5 \times 10^{17}\text{GeV}$. Interestingly, existence of such ULA species is not favored by the CMB observations in the standard cosmology. It is the inclusion of EDE that lifts the CMB-lockdown on such ULA. Furthermore, we found such ULA can alleviate the tension between AdS-EDE and LSS data, yielding $H_0 = 72.53_{-0.58}^{+0.51}$ and $S_8 = 0.785_{-0.016}^{+0.015}$, both within 1σ range of the locally measured values. There is still residual inconsistency between AdS-EDE+ULA and the EFT likelihood, highlighting the importance of more precise full shape matter power spectrum data, e.g. DES-Y3 [36], in studying DM and EDE, which might worth further research in future studies.

It is interesting that $r_a \sim 6\%$ always implies $f_a \sim 10^{17}\text{GeV}$ (despite the axion mass or thawing time), which fits well with the string theory expectation [45, 46], and AdS vacua are also ubiquitous in string landscape [87], see also [88]. Furthermore, in addition to the 10^{-26}eV ULA, the EDE itself might be realized by 10^{-27}eV ULA by exploiting the weak

gravity conjecture [89]. Thus how to embed relevant models into a UV-complete theory will be worth exploring, see e.g [90, 91]. In Ref.[22], it has been found that in the pre-recombination solutions of the Hubble tension, the shift of primordial scalar spectral index scales as $\delta n_s \simeq 0.4 \frac{\delta H_0}{H_0}$, which seems to suggest a scale-invariant Harrison-Zeldovich spectrum ($n_s = 1$) for $H_0 \sim 73\text{km/s/Mpc}$. Here, we confirm this result again, see Tables-I, which might have radical implications on our understanding of the primordial Universe.

Acknowledgments This work is supported by NSFC, Nos.12075246, 11690021. Some figures in this paper are plotted with the help of GetDist [92]. The computations are performed on the TianHe-II supercomputer and the Xmaris cluster. We thank Alessandra Silvestri for useful comments and discussions.

Appendix A: More MCMC results

1. Results without S_8 and/or M_B prior

Denoting Planck18+BAOLZ+SNIa+EFT as D_1 , we add the S_8 , M_B prior or both as D_2 to see their effects on parameter constraints in the AdS-EDE+ULA model with $m_a \simeq 1.8h \times 10^{-26}\text{eV}$ and $\alpha_{ads} = 3.79 \times 10^{-4}$ and compute the Q_{DMAP} values. Posterior distributions and bestfit values are shown in Fig.6 and Table.III while Table.IV reports the corresponding bestfit χ^2 per dataset. The results imply that the S_8 prior is crucial in the detection of ULA. This is to be expected, because though EDE opens up the parameter space for ULA, it does not require the existence of ULA since EDE models alone are known to be compatible with CMB+SNIa+BAO. It is the inclusion of S_8 information that sets the "need" for ULA due to the exacerbated S_8 tension in original EDE models.

2. Results of varying model parameters m_a , Θ_i and α_{ads}

In the main text we fixed three model parameters $\{m_a, \Theta_i, \alpha_{ads}\}$ of AdS-EDE+ULA due to convergence or volume effect reasons. To illustrate their effects on cosmological parameters, in this subsection we present MCMC results of AdS-EDE+ULA with m_a , Θ_i and α_{ads} letting free to vary one by one. Due to the considerably prolonged convergence time, we use the dataset Planck18+fsBAO+SNIa+ S_8 + M_B excluding the slow EFT data. As noted in the main text and Tab.I, this dataset produces very similar cosmological constraints

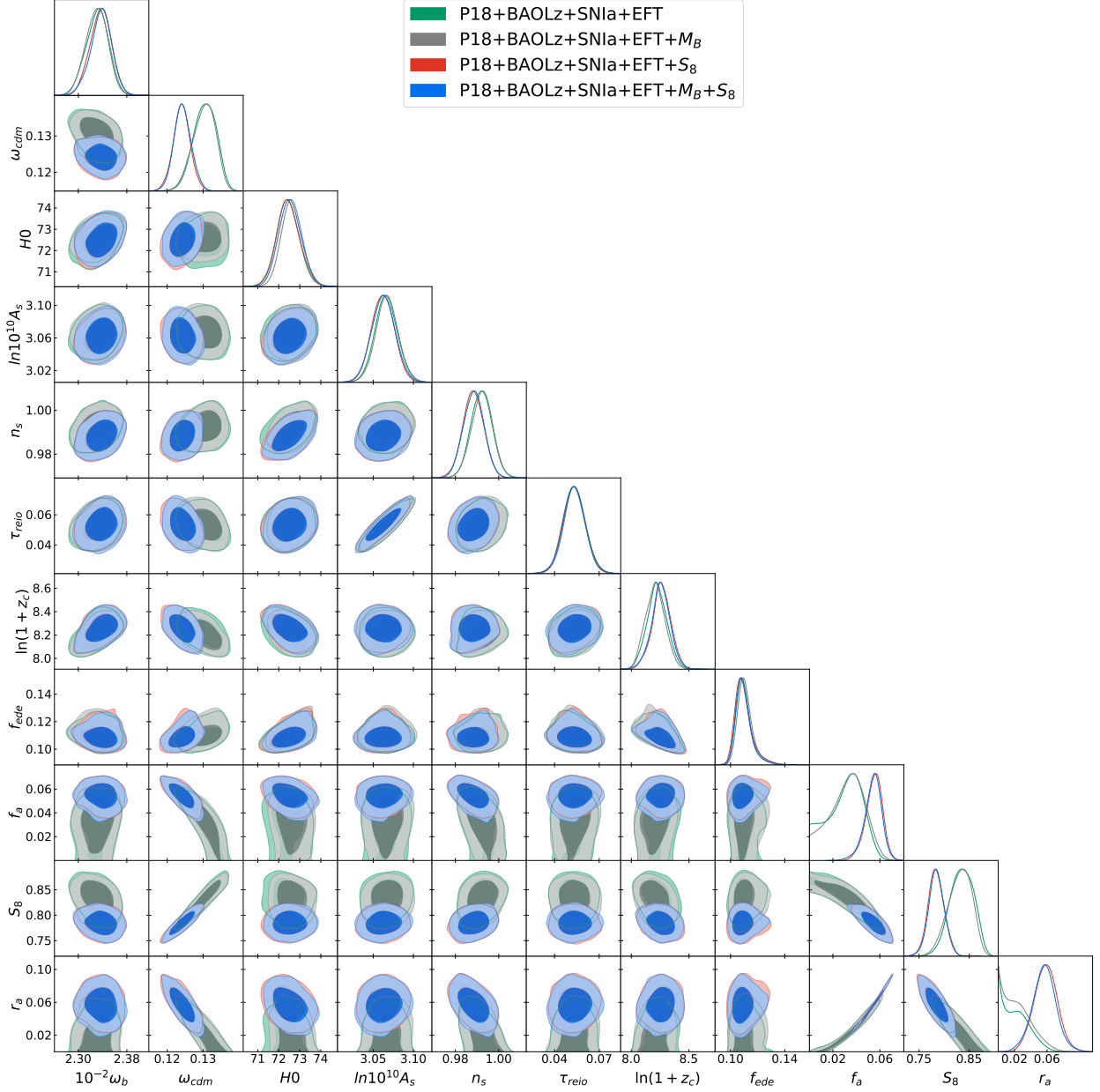


FIG. 6: 68% and 95% posterior distribution of cosmological parameters in AdS-EDE+ULA with and without S_8 and/or M_B prior.

as that with EFT but runs much faster. We use flat priors on $\{m_a, \Theta_i, \alpha_{ads}\}$, see Tab.V. We constrain axion mass m_a to roughly the mass range $10^{-24} \sim 10^{-28} \text{eV}$ which is wide enough to cover the interesting mass range $\mathcal{O}(10^{-26} \text{eV}) \gtrsim m_a \gtrsim \mathcal{O}(10^{-27} \text{eV})$ as argued in section-III and also excludes regions where the scalar field behaves like (early) dark energy or is degenerate with cold dark matter. For initial phase Θ_i we exclude the extreme values near 0 or π . For α_{ads} we set a small lower bound so that we are sampling models with an

	D_1	$D_1 + M_B$	$D_1 + S_8$	$D_1 + M_B + S_8$
100 ω_b	$2.331(2.329)^{+0.020}_{-0.017}$	$2.331(2.327) \pm 0.018$	$2.337(2.342) \pm 0.018$	$2.338(2.331)^{+0.018}_{-0.016}$
ω_{cdm}	$0.1305(0.1312)^{+0.0034}_{-0.0029}$	$0.1303(0.1312)^{+0.0036}_{-0.0027}$	$0.1241(0.1231) \pm 0.0024$	$0.1242(0.1229)^{+0.0023}_{-0.0025}$
H_0	$72.44(72.45) \pm 0.53$	$72.62(72.44) \pm 0.49$	$72.46(72.24)^{+0.49}_{-0.57}$	$72.53(72.14)^{+0.51}_{-0.58}$
$\ln 10^{10} A_s$	$3.066(3.069) \pm 0.014$	$3.067(3.069) \pm 0.014$	$3.062(3.059) \pm 0.014$	$3.063(3.066)^{+0.014}_{-0.015}$
n_s	$0.9921(0.9958) \pm 0.0049$	$0.9923(0.9959) \pm 0.0048$	$0.9882(0.989) \pm 0.0048$	$0.9885(0.9856)^{+0.0048}_{-0.0048}$
τ_{reio}	$0.0529(0.057) \pm 0.0072$	$0.0536(0.057) \pm 0.0073$	$0.0532(0.0501) \pm 0.0073$	$0.0534(0.0549)^{+0.007}_{-0.0076}$
$\ln(1 + z_c)$	$8.225(8.213) \pm 0.089$	$8.207(8.213) \pm 0.084$	$8.261(8.307)^{+0.082}_{-0.11}$	$8.255(8.256)^{+0.088}_{-0.069}$
f_{ede}	$0.1098(1.054)^{+0.0038}_{-0.0060}$	$0.1111(0.1053)^{+0.0034}_{-0.0067}$	$0.1095(0.101)^{+0.0037}_{-0.0071}$	$0.1094(0.1124)^{+0.0036}_{-0.0064}$
f_a/M_p	$0.031(0.024)^{+0.019}_{-0.011}$	$0.032(0.024)^{+0.017}_{-0.012}$	$0.0550(0.0596)^{+0.0076}_{-0.0059}$	$0.0541(0.0631)^{+0.0081}_{-0.0057}$
r_a	$< 0.029(0.011)$	$< 0.031(0.011)$	$0.058(0.0668) \pm 0.014$	$0.0567(0.0751)^{+0.015}_{-0.013}$
M_B	$-19.274(-19.275) \pm 0.015$	$-19.269(-19.275) \pm 0.014$	$-19.274(-19.28)^{+0.013}_{-0.015}$	$-19.27(-19.28)^{+0.014}_{-0.016}$
S_8	$0.835(0.847)^{+0.026}_{-0.022}$	$0.832(0.847)^{+0.027}_{-0.020}$	$0.784(0.777) \pm 0.016$	$0.785(0.772)^{+0.015}_{-0.016}$
Ω_m	$0.2998(0.2976) \pm 0.0055$	$0.2983(0.2975) \pm 0.0052$	$0.2983(0.3009) \pm 0.0054$	$0.2975(0.3037)^{+0.0053}_{-0.0057}$

TABLE III: 68%C.L. posterior constraints or 95%C.L. upper bounds on cosmological parameters in AdS-EDE+ULA. D_1 denotes the dataset Planck18+BAOLz+SNIa+EFT.

AdS phase but variable depth. Note that models with α_{ads} free to take both positive and negative values have been studied in Ref.[21] and it is concluded the existence of the AdS phase is weakly hinted. Posterior distributions of cosmological parameters after releasing $\{m_a, \Theta_i, \alpha_{ads}\}$ separately are plotted in Fig.7, Fig.8 and Fig.9. For all plots we also include the AdS-EDE+ULA with $\{m_a, \Theta_i, \alpha_{ads}\}$ fixed to their values in the main text (i.e. the last column of Tab.I) as reference.

Fig.7 plots the results of varying Θ_i . ULA fraction r_a is determined by its initial energy fraction at thawing to a good extent because after that ULA energy density redshifts just as matter. Since data constrained r_a to a specific range, it is expected that f_a and Θ_i are strongly anti-correlated when m_a fixed because the energy fraction at thawing is proportional to $V(\Theta_i) = m_a^2 f_a^2 (1 - \cos \Theta_i)$. According to Fig.7, the data constraint on r_a is robust against varying Θ_i . r_a only constrains the value of a specific combination of f_a and Θ_i when m_a is fixed, thus Θ_i and f_a alone are poorly constrained because of the strong anti-correlation. Fixing Θ_i amounts to picking out a specific value of f_a and does not bias our conclusion about

	D_1	$D_1 + M_B$	$D_1 + S_8$	$D_1 + M_B + S_8$
Planck18 high- l TTTEEE	2350.43	2350.54	2353.9	2352.72
Planck18 low- l TT	20.11	20.14	20.55	20.71
Planck18 low- l EE	396.25	396.26	395.78	396.06
Planck18 lensing	9.95	9.98	9.79	9.82
Pantheon	1026.69	1026.69	1026.88	1026.94
BAO low z	2.09	2.10	1.75	1.53
eft withbao highzNGC	66.98	66.95	68.85	69.72
eft withbao highzSGC	63.23	63.27	60.89	60.73
eft withbao lowzNGC	70.64	70.67	71.24	71.26
S_8	-	-	1.22	1.18
M_B	-	0.65	-	0.79
χ_{CMB}^2	2776.74	2776.92	2780.02	2779.31
χ_{EFT}^2	200.85	200.89	200.98	201.71
χ_{tot}^2	4006.36	4007.26	4010.85	4011.46

TABLE IV: Bestfit χ^2 per dataset for AdS-EDE+ULA. D_1 denotes Planck18+BAOLz+SNiA+EFT.

Parameter	Prior
$10^{-6}m_a/H_0$	$[10^{-1}, 10^2]$
Θ_i	$[0.15, 3]$
$10^4\alpha_{ads}$	> 0.1

TABLE V: Flat priors on $\{m_a, \Theta_i, \alpha_{ads}\}$.

r_a .

Fig.8 plots the results of varying m_a . Similar to the case of Θ_i , varying m_a relaxes the constraints on f_a because $V(\Theta_i) \propto m_a^2 f_a^2$. What is different is that constraints on r_a is no longer stable against varying m_a . This is to be expected given the arguments in the main text that EDE only opens the parameter space for ULA in the mass range $\mathcal{O}(10^{-26}\text{eV}) \gtrsim m_a \gtrsim \mathcal{O}(10^{-27}\text{eV})$ and the results of Ref.[58, 59]. Moreover, the heavier ULA is, the more degenerate it is with CDM for the datasets we considered, thus the m_a

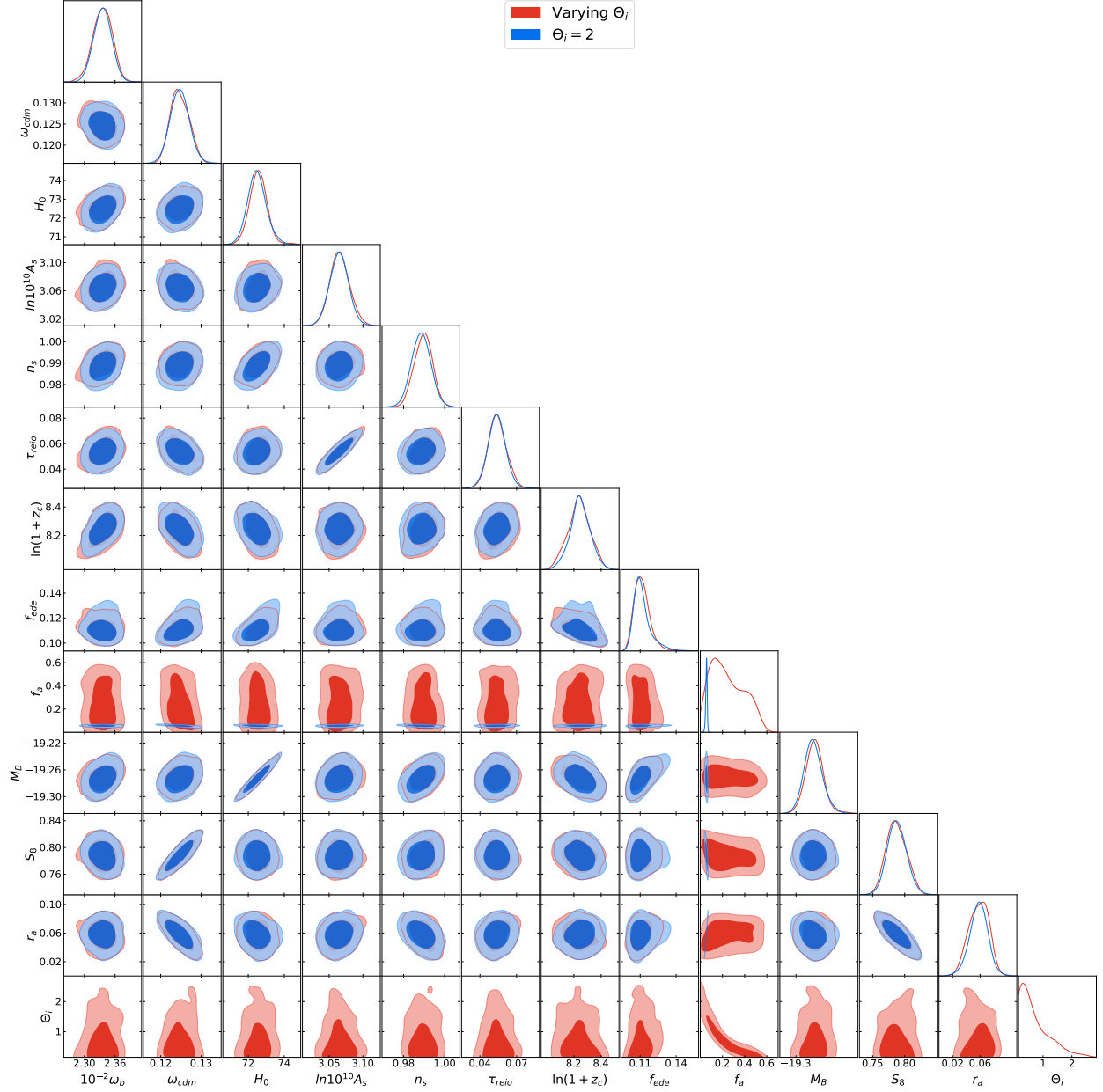


FIG. 7: 68% and 95% posterior distribution of cosmological parameters in AdS-EDE+ULA with initial ULA configuration Θ_i varied.

distribution shows a long tail in the high mass range. In turn, when ULA is indistinguishable from CDM, large portion of CDM can be replaced by ULA which is also reflected in Fig.8 as relaxed bounds on r_a and ω_{cdm} and anti-correlation between them.

Fig.9 plots the results of varying α_{ads} . Fig.10 and Table.VI further compares AdS-EDE+ULA with $\alpha_{ads} = 0$ (no AdS phase, rolling EDE potential) and $\alpha_{ads} = 3.79 \times 10^{-4}$ in terms of constraints on relevant cosmological parameters and bestfit χ^2 . Despite fitting

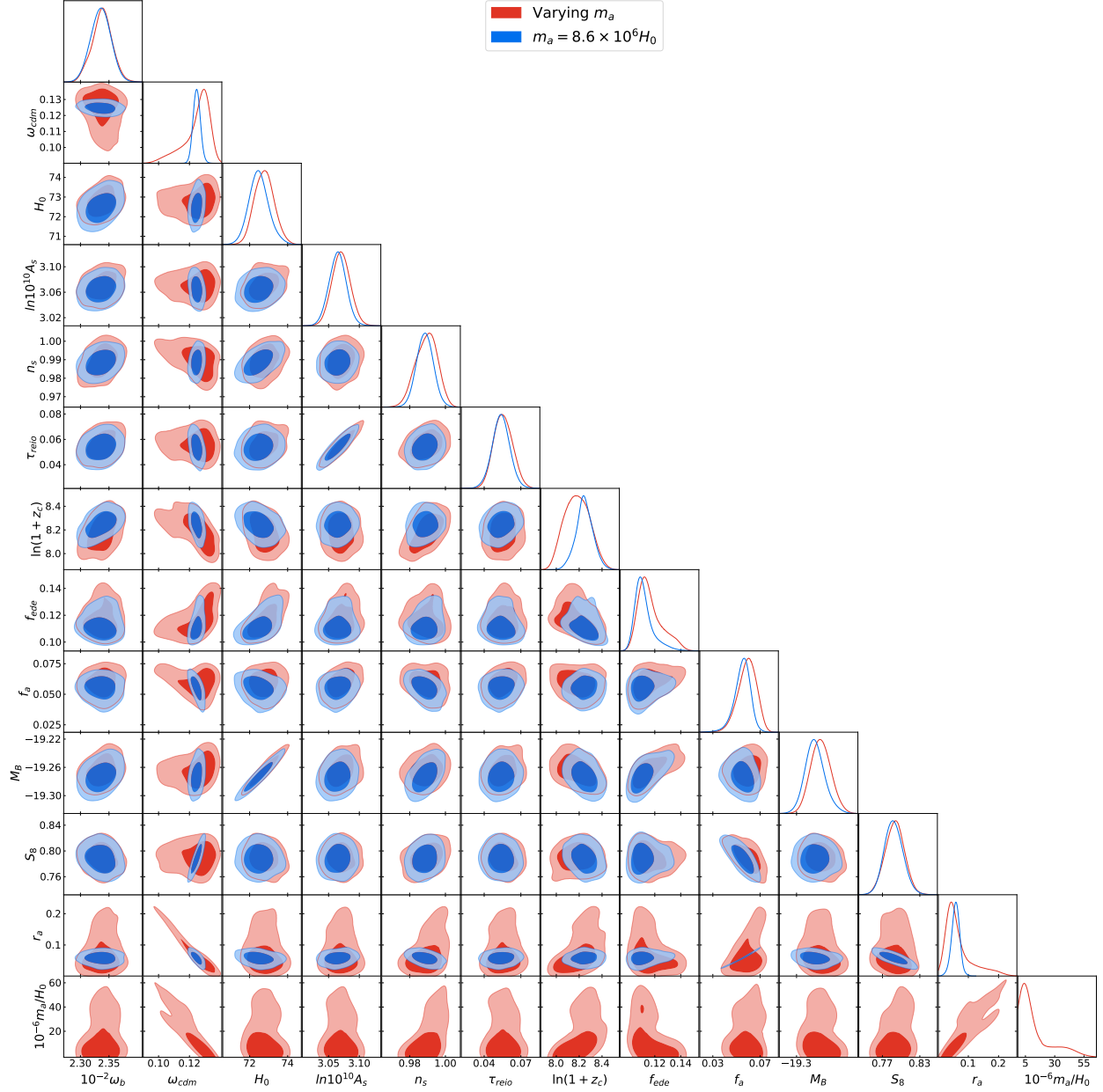


FIG. 8: 68% and 95% posterior distribution of cosmological parameters in AdS-EDE+ULA with ULA mass m_a varied.

the local Hubble measurement better without worsening the overall fit, models with non-negligible AdS phase is punished by the phase space volume effect. Non-zero α_{ads} value puts a theoretical lower bound on f_{ede} and cuts out part of the viable parameter space due to the fact that the field would be trapped in the disastrous negative energy region if f_{ede} becomes too small. Thus the smaller α_{ads} is, the larger the viable phase space is. As a result, MCMC chain will tend to explore points near $\alpha_{ads} = 0$ despite better fit at $\alpha_{ads} \neq 0$, making AdS

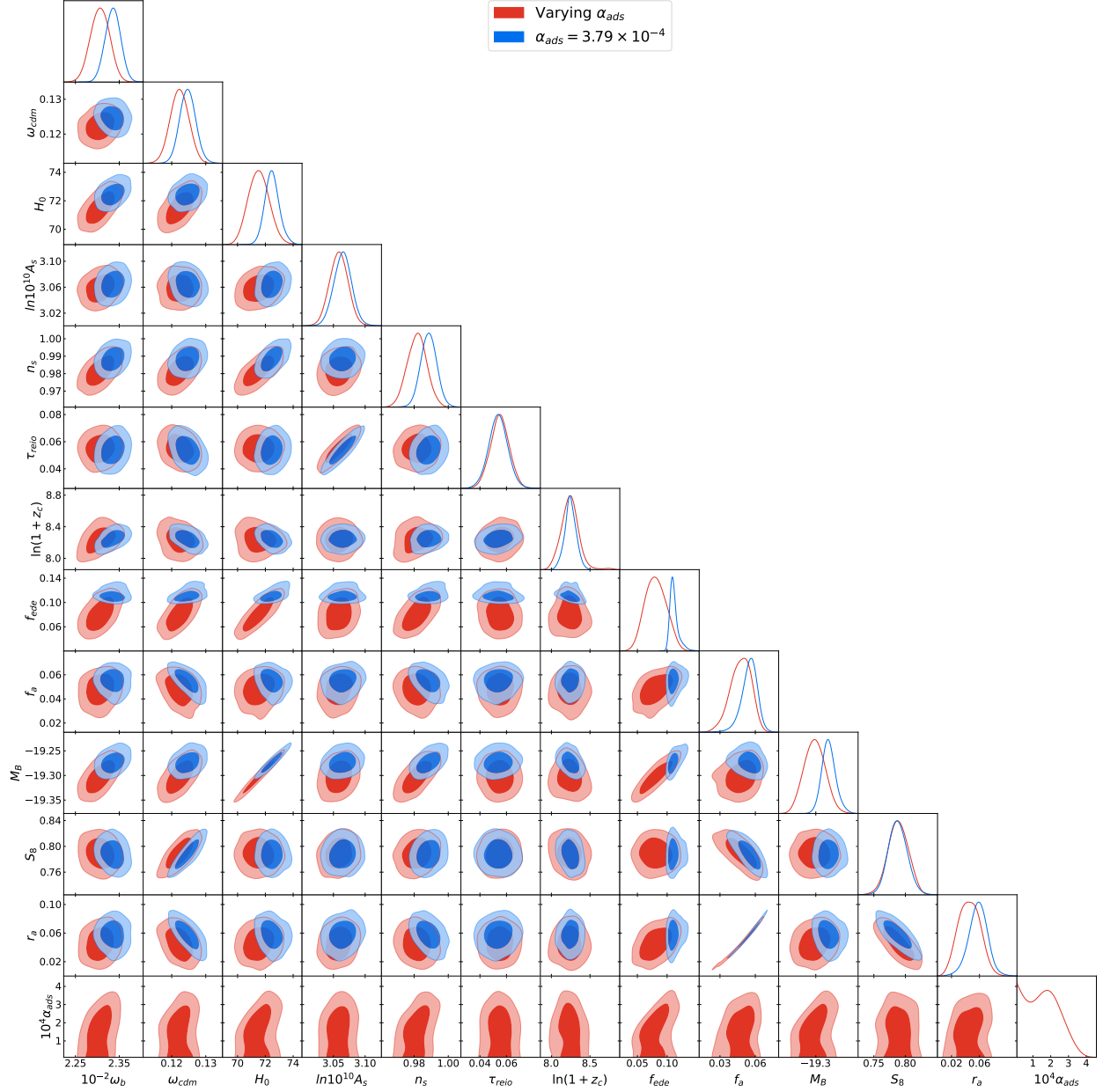


FIG. 9: 68% and 95% posterior distribution of cosmological parameters in AdS-EDE+ULA with AdS relative depth α_{ads} varied.

only weakly hinted. Fig.9 is also compatible with the results of Ref.[21]. Constraints on r_a is less strict when α_{ads} is let free to vary or fixed to 0 but the 95% C.L. detection conclusion is unchanged. As argued in the main text, it is EDE that opens up the parameter space for ULA. Thus the higher f_{ede} the more ULA is allowed. Because the existence of an AdS phase increases f_{ede} , it also increases the allowed ULA fraction r_a . However, since α_{ads} is not directly related to the mechanism that opens up ULA parameter space, it is thus not

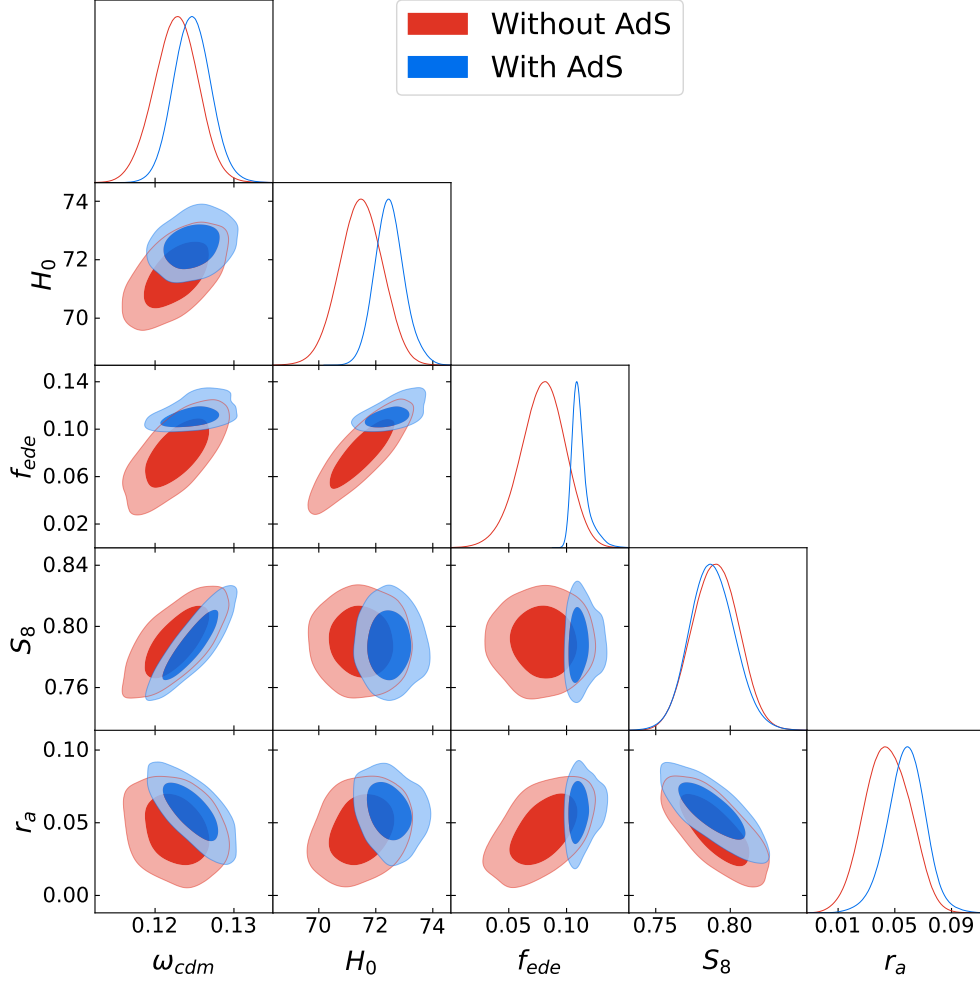


FIG. 10: 68% and 95% posterior distribution of cosmological parameters in AdS-EDE+ULA with and without an AdS phase.

Dataset	$\alpha_{ads} = 0$	$\alpha_{ads} = 3.79 \times 10^{-4}$
Planck18	2777.43	2781.03
Pantheon	1026.48	1026.89
fsBAO	8.03	9.25
S_8	4.27	1.06
M_B	2.89	0.12
χ^2_{tot}	3819.09	3818.35

TABLE VI: Bestfit χ^2 for AdS-EDE+ULA with $\alpha_{ads} = 0$ and $\alpha_{ads} = 3.79 \times 10^{-4}$.

required by the detection of ULA at 95%C.L.

- [1] N. Aghanim et al. (Planck), *Astron. Astrophys.* **641**, A6 (2020), 1807.06209.
- [2] A. G. Riess, S. Casertano, W. Yuan, J. B. Bowers, L. Macri, J. C. Zinn, and D. Scolnic, *Astrophys. J. Lett.* **908**, L6 (2021), 2012.08534.
- [3] S. Birrer et al., *Astron. Astrophys.* **643**, A165 (2020), 2007.02941.
- [4] W. L. Freedman, *Astrophys. J.* **919**, 16 (2021), 2106.15656.
- [5] L. Verde, T. Treu, and A. G. Riess, *Nature Astron.* **3**, 891 (2019), 1907.10625.
- [6] L. Knox and M. Millea, *Phys. Rev. D* **101**, 043533 (2020), 1908.03663.
- [7] E. Di Valentino, A. Melchiorri, and J. Silk, *Nature Astron.* **4**, 196 (2019), 1911.02087.
- [8] W. Handley, *Phys. Rev. D* **103**, L041301 (2021), 1908.09139.
- [9] T. Karwal and M. Kamionkowski, *Phys. Rev. D* **94**, 103523 (2016), 1608.01309.
- [10] V. Poulin, T. L. Smith, T. Karwal, and M. Kamionkowski, *Phys. Rev. Lett.* **122**, 221301 (2019), 1811.04083.
- [11] P. Agrawal, F.-Y. Cyr-Racine, D. Pinner, and L. Randall (2019), 1904.01016.
- [12] M.-X. Lin, G. Benevento, W. Hu, and M. Raveri, *Phys. Rev. D* **100**, 063542 (2019), 1905.12618.
- [13] S. Alexander and E. McDonough, *Phys. Lett. B* **797**, 134830 (2019), 1904.08912.
- [14] T. L. Smith, V. Poulin, and M. A. Amin, *Phys. Rev. D* **101**, 063523 (2020), 1908.06995.
- [15] F. Niedermann and M. S. Sloth, *Phys. Rev. D* **103**, L041303 (2021), 1910.10739.
- [16] J. Sakstein and M. Trodden, *Phys. Rev. Lett.* **124**, 161301 (2020), 1911.11760.
- [17] G. Ye and Y.-S. Piao, *Phys. Rev. D* **101**, 083507 (2020), 2001.02451.
- [18] G. Ballesteros, A. Notari, and F. Rompineve, *JCAP* **11**, 024 (2020), 2004.05049.
- [19] M. Braglia, W. T. Emond, F. Finelli, A. E. Gumrukcuoglu, and K. Koyama, *Phys. Rev. D* **102**, 083513 (2020), 2005.14053.
- [20] A. Chudaykin, D. Gorbunov, and N. Nedelko, *JCAP* **08**, 013 (2020), 2004.13046.
- [21] G. Ye and Y.-S. Piao, *Phys. Rev. D* **102**, 083523 (2020), 2008.10832.
- [22] G. Ye, B. Hu, and Y.-S. Piao (2021), 2103.09729.
- [23] A. Chudaykin, D. Gorbunov, and N. Nedelko, *Phys. Rev. D* **103**, 043529 (2021), 2011.04682.
- [24] M.-X. Lin, W. Hu, and M. Raveri, *Phys. Rev. D* **102**, 123523 (2020), 2009.08974.

- [25] V. I. Sabla and R. R. Caldwell, *Phys. Rev. D* **103**, 103506 (2021), 2103.04999.
- [26] S. Nojiri, S. D. Odintsov, D. Saez-Chillon Gomez, and G. S. Sharov, *Phys. Dark Univ.* **32**, 100837 (2021), 2103.05304.
- [27] T. Karwal, M. Raveri, B. Jain, J. Khoury, and M. Trodden (2021), 2106.13290.
- [28] M. Braglia, M. Ballardini, W. T. Emond, F. Finelli, A. E. Gumrukcuoglu, K. Koyama, and D. Paoletti, *Phys. Rev. D* **102**, 023529 (2020), 2004.11161.
- [29] M. Ballardini, M. Braglia, F. Finelli, D. Paoletti, A. A. Starobinsky, and C. Umiltà, *JCAP* **10**, 044 (2020), 2004.14349.
- [30] M. Braglia, M. Ballardini, F. Finelli, and K. Koyama, *Phys. Rev. D* **103**, 043528 (2021), 2011.12934.
- [31] E. Di Valentino, O. Mena, S. Pan, L. Visinelli, W. Yang, A. Melchiorri, D. F. Mota, A. G. Riess, and J. Silk (2021), 2103.01183.
- [32] L. Perivolaropoulos and F. Skara (2021), 2105.05208.
- [33] M. Asgari et al., *Astron. Astrophys.* **634**, A127 (2020), 1910.05336.
- [34] M. Asgari et al. (KiDS), *Astron. Astrophys.* **645**, A104 (2021), 2007.15633.
- [35] C. Heymans et al., *Astron. Astrophys.* **646**, A140 (2021), 2007.15632.
- [36] T. M. C. Abbott et al. (DES) (2021), 2105.13549.
- [37] R. C. Nunes and S. Vagnozzi, *Mon. Not. Roy. Astron. Soc.* **505**, 5427 (2021), 2106.01208.
- [38] J. C. Hill, E. McDonough, M. W. Toomey, and S. Alexander, *Phys. Rev. D* **102**, 043507 (2020), 2003.07355.
- [39] M. M. Ivanov, E. McDonough, J. C. Hill, M. Simonović, M. W. Toomey, S. Alexander, and M. Zaldarriaga, *Phys. Rev. D* **102**, 103502 (2020), 2006.11235.
- [40] G. D'Amico, L. Senatore, P. Zhang, and H. Zheng, *JCAP* **05**, 072 (2021), 2006.12420.
- [41] K. Jedamzik, L. Pogosian, and G.-B. Zhao, *Commun. in Phys.* **4**, 123 (2021), 2010.04158.
- [42] J.-Q. Jiang and Y.-S. Piao (2021), 2107.07128.
- [43] S. Vagnozzi (2021), 2105.10425.
- [44] L. Pogosian, G.-B. Zhao, and K. Jedamzik, *Astrophys. J. Lett.* **904**, L17 (2020), 2009.08455.
- [45] P. Svrcek and E. Witten, *JHEP* **06**, 051 (2006), hep-th/0605206.
- [46] A. Arvanitaki, S. Dimopoulos, S. Dubovsky, N. Kaloper, and J. March-Russell, *Phys. Rev. D* **81**, 123530 (2010), 0905.4720.
- [47] L. Hui (2021), 2101.11735.

- [48] H. Davoudiasl and P. B. Denton, Phys. Rev. Lett. **123**, 021102 (2019), 1904.09242.
- [49] Y. Chen, J. Shu, X. Xue, Q. Yuan, and Y. Zhao, Phys. Rev. Lett. **124**, 061102 (2020), 1905.02213.
- [50] R. Brito, S. Ghosh, E. Barausse, E. Berti, V. Cardoso, I. Dvorkin, A. Klein, and P. Pani, Phys. Rev. Lett. **119**, 131101 (2017), 1706.05097.
- [51] C. Palomba et al., Phys. Rev. Lett. **123**, 171101 (2019), 1909.08854.
- [52] J. Zhang and H. Yang, Phys. Rev. D **99**, 064018 (2019), 1808.02905.
- [53] J. Zhang and H. Yang, Phys. Rev. D **101**, 043020 (2020), 1907.13582.
- [54] L. Sagunski, J. Zhang, M. C. Johnson, L. Lehner, M. Sakellariadou, S. L. Liebling, C. Palenzuela, and D. Neilsen, Phys. Rev. D **97**, 064016 (2018), 1709.06634.
- [55] J. Huang, M. C. Johnson, L. Sagunski, M. Sakellariadou, and J. Zhang, Phys. Rev. D **99**, 063013 (2019), 1807.02133.
- [56] J. Zhang, Z. Lyu, J. Huang, M. C. Johnson, L. Sagunski, M. Sakellariadou, and H. Yang (2021), 2105.13963.
- [57] I. J. Allali, M. P. Hertzberg, and F. Rompineve (2021), 2104.12798.
- [58] R. Hlozek, D. J. E. Marsh, and D. Grin, Mon. Not. Roy. Astron. Soc. **476**, 3063 (2018), 1708.05681.
- [59] A. Laguë, J. R. Bond, R. Hložek, K. K. Rogers, D. J. E. Marsh, and D. Grin (2021), 2104.07802.
- [60] W. Hu, R. Barkana, and A. Gruzinov, Phys. Rev. Lett. **85**, 1158 (2000), astro-ph/0003365.
- [61] J.-c. Hwang and H. Noh, Phys. Lett. B **680**, 1 (2009), 0902.4738.
- [62] D. J. E. Marsh and P. G. Ferreira, Phys. Rev. D **82**, 103528 (2010), 1009.3501.
- [63] L. W. Fung, L. Li, T. Liu, H. N. Luu, Y.-C. Qiu, and S. H. H. Tye (2021), 2102.11257.
- [64] L. W. Fung, L. Li, T. Liu, H. N. Luu, Y.-C. Qiu, and S. H. H. Tye (2021), 2105.01631.
- [65] B. Audren, J. Lesgourgues, K. Benabed, and S. Prunet, JCAP **02**, 001 (2013), 1210.7183.
- [66] T. Brinckmann and J. Lesgourgues, Phys. Dark Univ. **24**, 100260 (2019), 1804.07261.
- [67] J. Lesgourgues (2011), 1104.2932.
- [68] D. Blas, J. Lesgourgues, and T. Tram, JCAP **07**, 034 (2011), 1104.2933.
- [69] V. Poulin, T. L. Smith, D. Grin, T. Karwal, and M. Kamionkowski, Phys. Rev. D **98**, 083525 (2018), 1806.10608.
- [70] N. Aghanim et al. (Planck), Astron. Astrophys. **641**, A5 (2020), 1907.12875.

- [71] D. M. Scolnic et al., *Astrophys. J.* **859**, 101 (2018), 1710.00845.
- [72] F. Beutler, C. Blake, M. Colless, D. H. Jones, L. Staveley-Smith, L. Campbell, Q. Parker, W. Saunders, and F. Watson, *Mon. Not. Roy. Astron. Soc.* **416**, 3017 (2011), 1106.3366.
- [73] A. J. Ross, L. Samushia, C. Howlett, W. J. Percival, A. Burden, and M. Manera, *Mon. Not. Roy. Astron. Soc.* **449**, 835 (2015), 1409.3242.
- [74] D. Baumann, A. Nicolis, L. Senatore, and M. Zaldarriaga, *JCAP* **07**, 051 (2012), 1004.2488.
- [75] J. J. M. Carrasco, M. P. Hertzberg, and L. Senatore, *JHEP* **09**, 082 (2012), 1206.2926.
- [76] G. D’Amico, L. Senatore, and P. Zhang, *JCAP* **01**, 006 (2021), 2003.07956.
- [77] T. Colas, G. D’amico, L. Senatore, P. Zhang, and F. Beutler, *JCAP* **06**, 001 (2020), 1909.07951.
- [78] S. Alam et al. (BOSS), *Mon. Not. Roy. Astron. Soc.* **470**, 2617 (2017), 1607.03155.
- [79] P. Lemos, E. Lee, G. Efstathiou, and S. Gratton, *Mon. Not. Roy. Astron. Soc.* **483**, 4803 (2019), 1806.06781.
- [80] G. Benevento, W. Hu, and M. Raveri, *Phys. Rev. D* **101**, 103517 (2020), 2002.11707.
- [81] D. Camarena and V. Marra, *Mon. Not. Roy. Astron. Soc.* **504**, 5164 (2021), 2101.08641.
- [82] G. Efstathiou (2021), 2103.08723.
- [83] A. G. Riess et al. (2021), 2112.04510.
- [84] D. Scolnic et al. (2021), 2112.03863.
- [85] M. Raveri and W. Hu, *Phys. Rev. D* **99**, 043506 (2019), 1806.04649.
- [86] N. Schöneberg, G. Franco Abellán, A. Pérez Sánchez, S. J. Witte, V. Poulin, and J. Lesgourgues (2021), 2107.10291.
- [87] G. Obied, H. Ooguri, L. Spodyneiko, and C. Vafa (2018), 1806.08362.
- [88] S. K. Garg and C. Krishnan, *JHEP* **11**, 075 (2019), 1807.05193.
- [89] N. Kaloper, *Int. J. Mod. Phys. D* **28**, 1944017 (2019), 1903.11676.
- [90] D. J. E. Marsh, *Phys. Rev. D* **83**, 123526 (2011), 1102.4851.
- [91] D. J. E. Marsh, E. R. M. Tarrant, E. J. Copeland, and P. G. Ferreira, *Phys. Rev. D* **86**, 023508 (2012), 1204.3632.
- [92] A. Lewis (2019), 1910.13970.